



e-ISSN: 2278-8875
p-ISSN: 2320-3765

International Journal of Advanced Research

in Electrical, Electronics and Instrumentation Engineering

Volume 10, Issue 2, February 2021

ISSN INTERNATIONAL
STANDARD
SERIAL
NUMBER
INDIA

Impact Factor: 7.122

9940 572 462

6381 907 438

ijareeie@gmail.com

www.ijareeie.com



Performance Evaluation of Three-Phase VSI Fed IM Drive Using DFOC and IFOC

Jagriti Garg¹, R.S. Mandloi²

PG Student [P.E.], Dept. of EED, Shri G.S. Institute of Technology and Science, Madhya Pradesh, India¹

Assistant Professor, Dept. of EED, Shri G.S. Institute of Technology and Science, Madhya Pradesh, India²

ABSTRACT: Induction Motors have innumerable uses in the present world. Thus, it becomes a necessity to control IM speed with more efficiency and accuracy without any significant distortions. To achieve this, various control algorithms and techniques are implemented, so that the induction motor's performance can be controlled and enhanced. In this paper, two schemes of FOC i.e. Direct-Field Oriented control (DFOC) and Indirect-Field Oriented control (IFOC) developed on MATLAB/SIMULINK are compared based on their performance. In both the simulations, parameters implemented are same to validate and analyse which technique renders better control and performance for the induction motor. In both the simulation models, two PI controllers, one in speed control and other in FOC controller is implemented to get better response. These comparisons are performed on the basis of stator current, rotor speed, electromagnetic torque and total harmonic distortion (THD) of the induction motor.

KEYWORDS: Induction Motor, Field Oriented Control, Direct Field Oriented Control, Indirect Field Oriented Control, Total Harmonic Distortion.

I. INTRODUCTION

In today's world, electric motors have completely revolutionized the industrial world. Out of all the electric motors, induction motors are the most frequently used and hence have their own separate place in the industry [3]. The reason for its persistent use is that it has a simple and robust construction. That's why, it requires relatively lower maintenance, has higher reliability and involves cheaper operating and production costs. Therefore, several researches are being carried out for developing better techniques to control the performance of induction motors. Induction motor is completely based on electromagnetism. The main problem which arises with it is to control its speed so that low torque ripple, low THD, fast flux and torque response and parameters varying capability can be achieved. The control method used to control the speed of IM should be simple in structure and easy to tune.

Variable frequency drive is classified in two types of control one being Scalar and other being vector control. Vector control method is the most excellent method for induction motor's control [5] because it allows the control of frequency and voltage amplitude along with instantaneous position of voltage, current and flux due to which dynamic behaviour of the drive improves. The main objective of vector control is to control the torque and rotor flux of the motor independently, by estimating speed and voltage [9]. There are many vector control techniques of which Field oriented control is used in this paper. The propose of this paper is to control the speed of induction motor using the classification of FOC scheme i.e. Direct-FOC and Indirect-FOC in discrete system and compare them based on their performance analysis.

II. MATHEMATICAL MODEL OF INDUCTION MACHINE

To control the induction motor speed, control of flux and torque of the induction motor is desired in a stationary reference frame for better dynamic performance. In the FOC scheme, it is necessary to make the motor run at the maximum possible rpm to get better response from the motor. The stator field and rotor magnetic field should be orthogonal to each other to accomplish this.

The first point here is to measure the rotor angular position, from where the desired orientation of stator field vector is determined (this stator field vector needs to be at 90 degree to the rotor field vector). The second point is to control the three-phase current to achieve the desired stator field vector. In this control scheme, instead of dealing with the three-phase current directly, it has been converted into direct and quadrature current by using Clarke and Park transform. It's



Because for FOC dealing with ac currents having sinusoidal waveforms, it becomes hard to control ac signals through PID controllers. That’s why Clarke and Park transforms are used to translate the stationary stator reference frame into the rotating reference frame (d-q frame).

Electrical system of electrical machine (Induction motor) in d-q frame

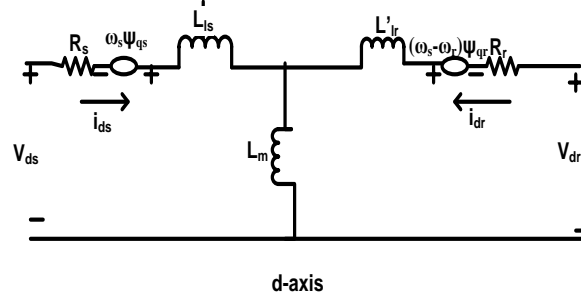


Fig. 1. Equivalent circuit of IM in d-axis

$$\left. \begin{aligned} V_{qs} &= R_s i_{qs} + \frac{d}{dt} (\psi_{qs}) + \omega_s \psi_{ds} \\ V_{ds} &= R_s i_{ds} + \frac{d}{dt} (\psi_{ds}) - \omega_s \psi_{qs} \\ V_{qr} &= R_r i_{qr} + \frac{d}{dt} (\psi_{qr}) + (\omega_s - \omega_r) \psi_{dr} \\ V_{dr} &= R_r i_{dr} + \frac{d}{dt} (\psi_{dr}) + (\omega_s - \omega_r) \psi_{qr} \end{aligned} \right\} \tag{1}$$

$$T_e = 1.5p (\psi_{ds} i_{qs} - \psi_{qs} i_{ds}) \tag{2}$$

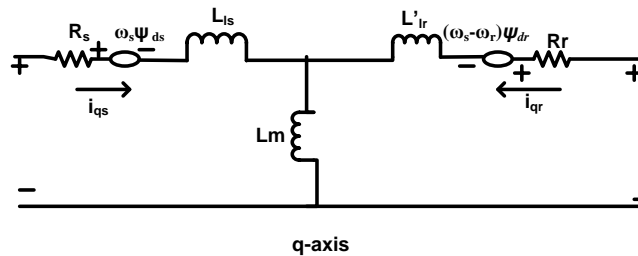


Fig. 2. Equivalent circuit of IM in q-axis

Where,

ω_r = rotor angular frequency

ω_s = stator angular frequency

$$\psi_{qs} = L_s i_{qs} + L_m i_{qr}$$

$$\psi_{ds} = L_s i_{ds} + L_m i_{dr}$$

$$\psi_{qr} = L_r i_{qr} + L_m i_{qs}$$

$$\psi_{dr} = L_r i_{dr} + L_m i_{ds}$$

$$L_s = L_{l_s} + L_m$$

$$L_r = L'_{l_r} + L_m$$

The rotor flux linkage is surmised to be on the d-axis to minimize the various variables in the equations above. Thus, after allying d-axis with phasor of rotor flux shall give,

$$\left. \begin{aligned} \psi_r &= \psi_{dr} \\ \psi_{qr} &= 0 \\ \frac{d}{dt} (\psi_{qr}) &= 0 \end{aligned} \right\} \tag{3}$$

Let, $\omega_{sl} = \omega_s - \omega_r$



Substituting (3) in (1) so,

$$\left. \begin{aligned} R_r i_{dr} + \frac{d}{dt} (\psi_r) &= 0 \\ R_r i_{qr} + \omega_{sl} \psi_r &= 0 \end{aligned} \right\} \tag{4}$$

From (1), (2) and (3) stator currents are,
Current which produces flux is,

$$i_{ds} = (1 + T_r \frac{d}{dt}) \frac{\psi_r}{L_m} \tag{5}$$

Current which produces torque is,

$$i_{qs} = \frac{T_r \psi_r \omega_{sl}}{L_m} \tag{6}$$

Where,

T_r = rotor time constant

Torque in d-q coordinates,

$$T_e = P \frac{L_m}{L_r} (\psi_{dr} i_{qs} - \psi_{qr} i_{ds}) \tag{7}$$

Substituting (5) and (6) in (7) electromagnetic torque equation is given by,

$$T_e = P \frac{L_m}{L_r} (\psi_{dr} i_{qs}) \tag{8}$$

P = no. of poles in induction motor

From (5), (6) and (8), it can be concluded that IM is completely transformed into equivalent separately excited DC motor [3].

III. FIELD ORIENTED CONTROL

FOC is a vector based controller. This controller makes the stator field direction to stay always orthogonal to the rotor field of the motor to produce the maximum torque so that motor performance improves. FOC scheme efficiently reduces the ripple of the system response and leads to a smoother operation of the motor.

In this research paper, three-phase induction motor’s performance are compared using two classifications of FOC, i.e. Direct FOC and Indirect FOC scheme fed by three phase VSI with PWM is developed. Here, IM is mathematically modelled in rotor flux orientation.

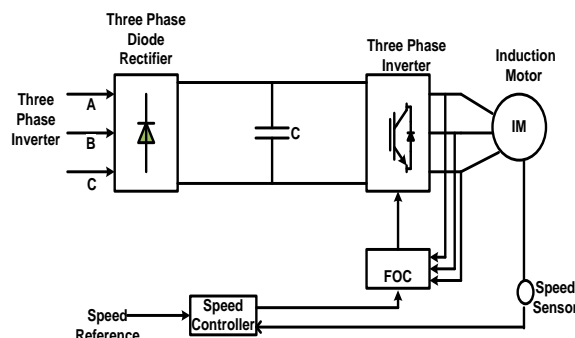


Fig. 3. Block Diagram of FOC IM drive fed by three-phase VSI

Here, Speed controller is the PI controller whose outputs are torque and flux which are applied to the FOC block as inputs.

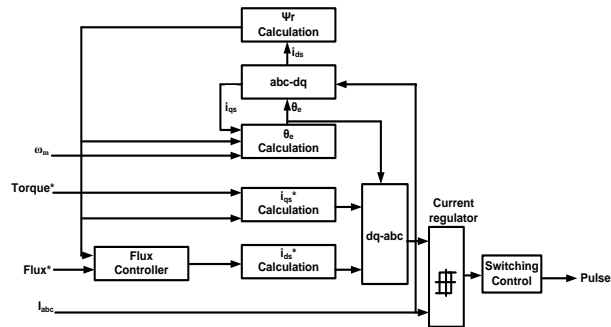


Fig. 4. Schematic Diagram of subsystem of FOC controller

Here, Ψ_r is rotor flux of the motor, θ_e is rotor flux rotating field’s phase angle, electromagnetic torque is calculated by using i_{qs}^* . This electromagnetic torque is computed by the torque reference and also the rotor flux that are utilized to calculate the q-axis component of stator current. i_{qs}^* is used to calculate the induction motor’s rotor flux, which is calculated by rotor flux reference to determine the stator current’s d-axis component.

(i) Direct Field Oriented Control Scheme

The synchronous reference’s position in the DFOC scheme depends upon the value of rotor flux linkages of d-q axes in the rotor reference frame. If the stationary reference frame’s position is assumed to be zero,

$$\begin{bmatrix} \psi'_{qr} \\ \psi'_{dr} \end{bmatrix} = \begin{bmatrix} \cos\theta_e & -\sin\theta_e \\ \sin\theta_e & \cos\theta_e \end{bmatrix} \begin{bmatrix} \psi_{qr}^s \\ \psi_{dr}^s \end{bmatrix} \tag{9}$$

To make $\psi'_{qr} = 0$ from (9), the position of synchronous frame is given by,

$$\theta_e = \text{angle}(\psi_{qr}^s - j\psi_{dr}^s) + \frac{\pi}{2} \tag{10}$$

$$\psi'_{dr} = \sqrt{(\psi_{qr}^s)^2 + (\psi_{dr}^s)^2} \tag{11}$$

From this approach, quantities like ψ_{qr}^s and ψ_{dr}^s are not directly measurable, so they are estimated by directly measuring the air-gap flux. Sensors are used to calculate the air-gap flux by positioning the sensors within the air-gap in the d-q axes of the stationary reference frame. It is done because the sensor’s arrangement in the stationary reference frame is fixed. The final outcome is that the peak magnitude d-q axes of air-gap flux linkage ψ_{qm}^s and ψ_{dm}^s are deemed as measurable in the stationary reference frame. Therefore, to determine ψ_{qr}^s and ψ_{dr}^s from ψ_{qm}^s and ψ_{dm}^s , note that,

$$\psi_{qm}^s = L_m(i_{qm}^s + i_{qr}^s) \tag{12}$$

$$i_{qr}^s = \frac{(\psi_{qm}^s - L_m i_{qs}^s)}{L_m} \tag{13}$$

The rotor flux linkage in q-axis can be stated as,

$$\psi_{qr}^s = L_{lr} i_{qr}^s + L_m(i_{qs}^s - i_{qr}^s) \tag{14}$$

By substituting (10) in (11), in the stationary reference frame’s d-q axes, rotor flux is,

$$\psi_{qr}^s = \frac{L'_{rr}}{L_m} \psi_{qm}^s - L'_{lr} i_{qs}^s \tag{15}$$

$$\psi_{dr}^s = \frac{L'_{rr}}{L_m} \psi_{dm}^s - L'_{lr} i_{ds}^s \tag{16}$$

Rotor flux calculator computes the d-axis flux linkage along with the position of the synchronous reference frame [1].

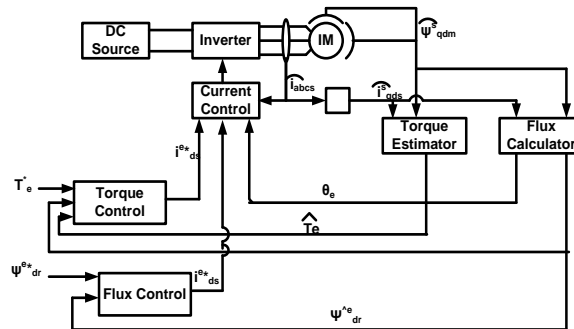


Fig. 5. Robust rotor field oriented control [1]

Torque control equation,

$$\psi_{qdr}^{\wedge e} = \frac{L'_{rr,est}}{L_{m,est}} \psi_{qdm}^{\wedge s} - L'_{lr,est} i_{qds}^{\wedge s} \tag{17}$$

Flux control equation,

$$i_{qs}^{e*} = \frac{T_e^*}{\frac{3}{2} \frac{P}{2} L_{m,est} \psi_{dr}^{\wedge e}} \tag{18}$$

Torque estimator equation,

$$\psi_{qds}^s = L_{ls} i_{qds}^s + \psi_{qdm}^s \tag{19}$$

In DFOC, three phase supply is given to the three-phase diode rectifier, which converts ac into dc, after getting dc supply, it is converted to an ac supply by using inverter. The connection between the rectifier and inverter has a DC link that protects the system from voltage anomaly or fluctuation. From the inverter, three phase voltage is then fed to the IM which produces the movement i.e. rotor speed.

Once the output rotor speed from the IM is determined, then it goes to the speed controller and the references are computed. The PI controller of the speed controller block produces flux and torque references for the FOC controller. Then the i_{abc}^* reference line currents corresponding to the torque and flux references is determined by the FOC controller.

This is then fed to the motor using a three-phase current regulator. Once the flux and torque signals are determined from the speed controller, then they are transformed into the space vector method in order to obtain the switching gate pulse as output. Then the magnetization control unit, which contains the switching logic, switches between the magnetization or normal operation mode. Meanwhile magnetization output with Park transformation is obtained. After that the pulse from FOC control is given to the three phase inverter and the cycle continues.

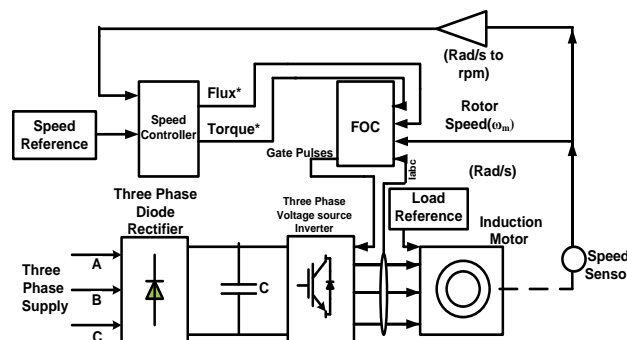


Fig. 6. Schematic diagram of Direct FOC in simulation



(ii) Indirect Field Oriented Control Scheme

The IFOC scheme differs from the DFOC scheme in the way so as to obtain the speed reference for field oriented controller. In IFOC, sensor speed output is not used after the IM. Instead the speed reference is obtained from a speed estimator with I_{abc} and V_{abc} as input. The model of IFOC is same as DFOC but with different speed management technique i.e. by using a speed estimator.

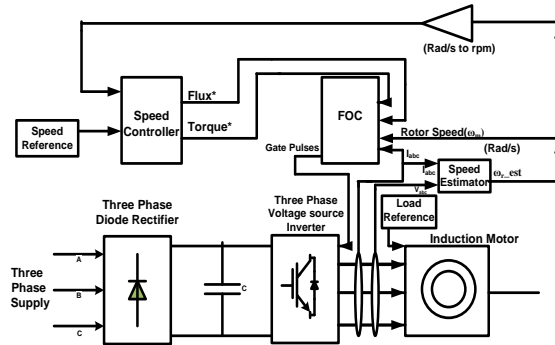


Fig. 7. Schematic diagram of Indirect FOC simulation

Speed Estimator-

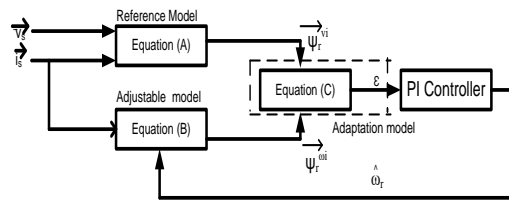


Fig. 8. Block diagram of MRAS-based speed estimator [6]

Induction motor’s speed estimation using the MRAS (model reference adaptive system) is estimated from measured terminal voltages and current. Then this estimated speed is utilized as a feedback in FOC system, therefore, without using the shaft mounted transducers, sensible speed control is achieved. Two different structures of machine model are used by speed estimator, to estimates the same motor state. The rotor flux vector is the primary used state variable. From Fig.8, the reference voltage of rotor flux model is given by (20).

$$p \begin{bmatrix} \psi_{ar}^{vi} \\ \psi_{\beta r}^{vi} \end{bmatrix} = \frac{L_r}{L_m} \begin{bmatrix} v_{\alpha s} \\ v_{\beta s} \end{bmatrix} \begin{bmatrix} R_s + \sigma L_s p & 0 \\ 0 & R_s + \sigma L_s p \end{bmatrix} \begin{bmatrix} i_{\alpha s} \\ i_{\beta s} \end{bmatrix} \tag{20}$$

The adjustable current of rotor flux model is given by (21).

$$p \begin{bmatrix} \psi_{ar}^{\omega i} \\ \psi_{\beta r}^{\omega i} \end{bmatrix} = \begin{bmatrix} -\frac{1}{T_r} & -\omega_r \\ \omega_r & -\frac{1}{T_r} \end{bmatrix} \begin{bmatrix} \psi_{ar}^{\omega i} \\ \psi_{\beta r}^{\omega i} \end{bmatrix} + \frac{L_m}{L_r} \begin{bmatrix} i_{\alpha s} \\ i_{\beta s} \end{bmatrix} \tag{21}$$

To tune the estimated speed, error signal (ϵ) is used and it is given by equation (22),

$$\epsilon = [\psi_{ar}^{\omega i} \psi_{\beta r}^{vi} - \psi_{\beta r}^{\omega i} \psi_{ar}^{vi}] \tag{22}$$

The phase difference between two vectors of estimated rotor flux, is used to change the estimated variable speed and, thus, for correcting the outcome of the adjustable model (21), as shown in Fig. 8. Where,

$\overline{\psi_r^{vi}} = [\psi_{ar}^{vi} \ \psi_{\beta r}^{vi}]^T$ is the rotor flux voltage model output and $\overline{\psi_r^{\omega i}} = [\psi_{ar}^{\omega i} \ \psi_{\beta r}^{\omega i}]^T$, is the output of the current model. And the stator voltage and current output are, $\overline{v_s} = [v_{\alpha s} \ v_{\beta s}]^T$ and $\overline{i_s} = [i_{\alpha s} \ i_{\beta s}]^T$



Where,

$$\text{Leakage factor } (\sigma) = 1 - L_m^2 / L_s L_r$$

$$p = \text{Differential operator } \frac{d}{dt}$$

$$T_r = \frac{L_r}{R_s} \text{ is the rotor time constant}$$

ω_r = rotor angular frequency.

Here the reference voltage model that is given by equation (21) and also shown in Fig. 8 is an open loop estimator of flux and that's why it is sensitive to variations in parameter, integration error and stator voltage estimation. The voltage estimation must involve entire non-linear reactions of the inverter, which are the dead-time of the switching device and the conducting voltage drop, to ensure stable function of this structure [6].

The MRAS based estimation of speed also relies on the adjustable flux model's correct performance (20), as shown in Fig.8. L_m^* and T_r^* parameters of this model must be revised with the main flux saturation level change. But the variation in the induced thermal drift must also be addressed in the case of only the T_r parameter. It is not possible to anticipate the thermal drift component of T_r drift, but it must be compensated by using the online parameter identification mechanism. The most favorable solution for T_r^* updates is to implement the feed forward compensation of flux-level related variations, which is in parallel with a robust error identification mechanism that tracks only the slow thermal drift changes in T_r . [6]

IV. SIMULATION RESULTS

The drive is operated under three different conditions. First, rotor speed at maximum load torque, second, variable rotor speed at constant load torque of 10Nm and then the third one is, rotor speed at variable load torque. The simulation outcomes include stator current, rotor speed and electromagnetic torque waves. Each parameter used in both the simulations of FOC schemes as shown in Fig.6 and Fig.7 are same. All the responses are taken with respect to time in seconds.

Table 1: Parameter of induction motor used in the DFOC and IFOC schemes

Parameters	Value
Power	6KW
Number of Poles	2
R_s	1.19 Ω
R_r	1.04 Ω
L_s	0.01759H
L_r	0.01759H
L_m	0.55H
Inertia, J	0.01 Kg m^2
Applied voltage	415 (Line to Line)
Friction Factor, F	0.0027
Frequency	50 Hz

Table 2: Proportional gain (K_p) and integral gain (K_i) of PI controller used in speed controller and FOC controller block

PI Controller	K_p	K_i
Speed control loop	0.7	0.1
Flux control loop	3	0.2



(i) Simulation result of DFOC

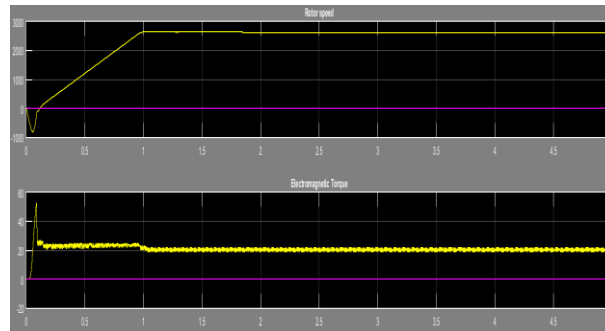


Fig. 9. Torque and rotor speed responses with speed command of 2800 rpm at maximum torque of 19.52 Nm.

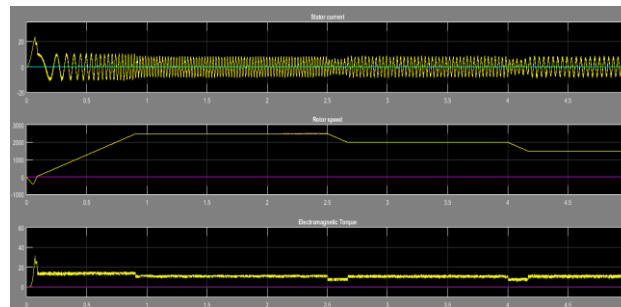


Fig. 10. Response of variable rotor speed of 2500, 2000 and 1500 rpm at 0sec, 2.5sec and 4 sec at constant load torque at 10 Nm

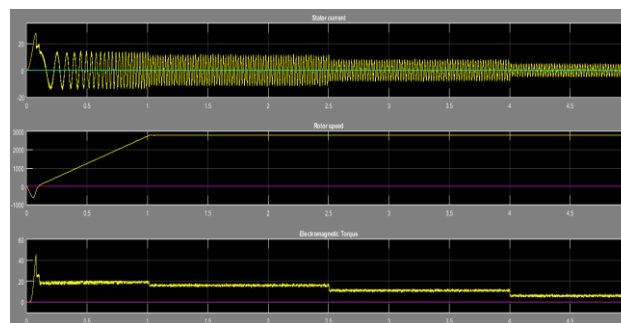


Fig. 11. Response of rotor speed at variable load torque of 15Nm, 10Nm and 5Nm at 0, 2.5 and 4 sec

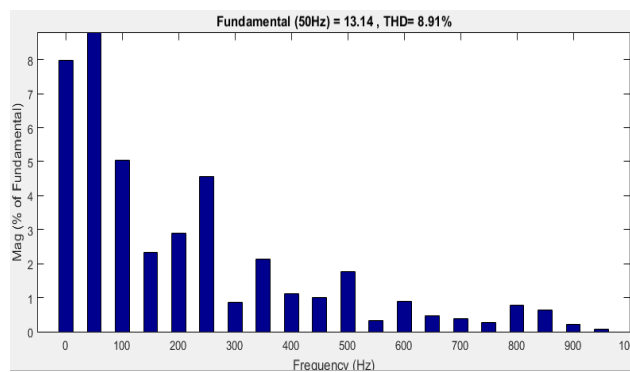


Fig. 12. THD of stator current in DFOC



From Fig. 9 it is observed that induction motor operates at its maximum load torque of 19.52Nm with speed command of 2800 rpm, after that rotor speed output observed is 2610 rpm. From Fig. 10., it can be seen that, after giving rotor command in decreasing order of 2500 rpm at 0 sec, 2000 rpm at 2.5 sec and 1500 rpm at 4 sec at the constant load torque of 10Nm, there is a slight decrease in stator current waveform at decreasing slope of rotor speed and also the electromagnetic torque is reduced at decreasing slope of rotor speed at 2.5 sec and 4 sec, after that the electromagnetic torque becomes constant to its commanded value. From Fig.11 by commanding three different load torques in decreasing order of 15Nm, 10Nm and 5 Nm at 0 sec, 2.5 sec and 4 sec, from that it is seen that as the load torque decreases, there is an increase in rotor speed and decrease in stator current waveform amplitudes. From all operating conditions, it is concluded that stator current changes corresponding to speed command and load torque. THD of stator current is 8.91% in DFOC as shown in Fig.12.

(ii) Simulation result for IFOC scheme

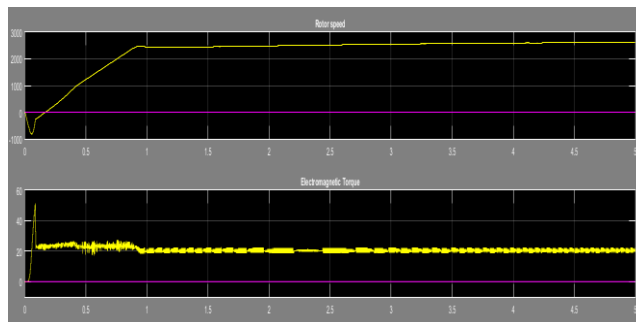


Fig. 13. Torque and rotor speed responses with speed command of 2800 rpm at maximum torque of 19.52 Nm

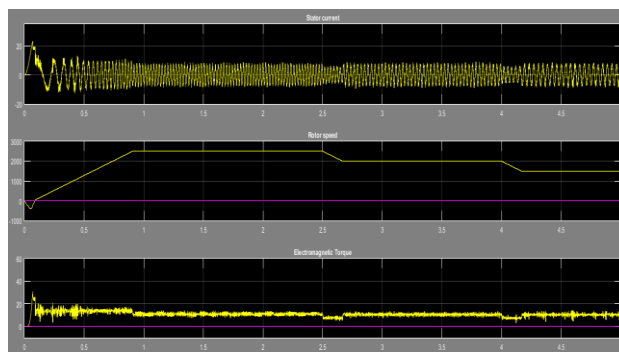


Fig. 14. Response of variable rotor speed of 2500, 2000 and 1500 rpm at 0 sec, 2.5 sec and 4 sec at constant load torque at 10 Nm

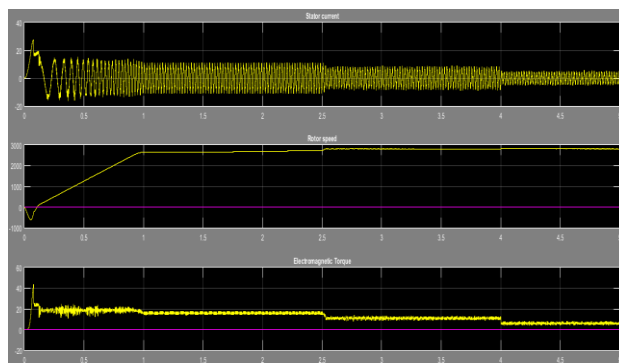


Fig. 15. Response of rotor speed at variable load torque of 15Nm, 10Nm and 5Nm at 0, 2.5 and 4sec

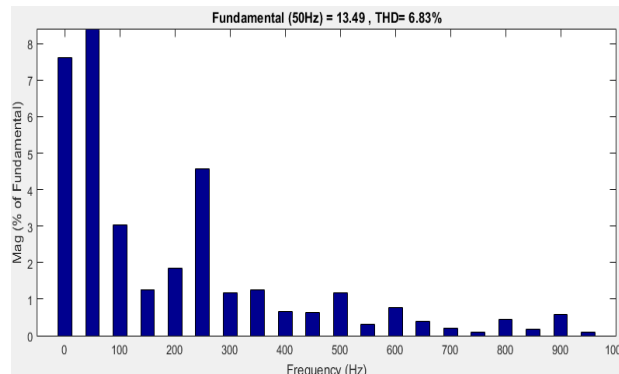


Fig. 16. THD of stator current in IFOC

From all the operating results of IFOC scheme, it is observed that the responses were overall almost same as the DFOC but in IFOC the settling time of rotor speed to become positive is marginally better i.e. 0.11 sec. But, in starting of electromagnetic torque waveform there are more ripples from 0 to 1 sec as compared to DFOC. However, THD of stator current is 6.83% at starting time 1.1.sec in IFOC scheme as shown in Fig.16.

Table 3: Comparison of DFOC and IFOC scheme

Attributes	DFOC	IFOC
Power	6KW	6KW
Rotor speed settling time	0.12sec	0.11sec
Rotor speed at maximum load	2610rpm	2666rpm
Accuracy	Comparatively Low	High
Parameter sensitivity	Less sensitive	Highly sensitive
Algorithm complexity	Less complex	More complex
Torque and flux ripples	Comparatively less	Less
Regulation	PI controller	PI controller
Current THD	8.91	6.83

Table 4: Settling time of the torque response

RPM	DFOC	IFOC
2800	0.145s	0.158s
1500	0.142s	0.148s
100	0.132s	0.136s



V. CONCLUSION

In this paper a fair comparison of three-phase VSI fed IM drive using two control strategies of FOC is given. The two schemes are DFOC and IFOC. The parameters implemented in both the schemes are same. After the performance analysis of both the models it is observed that the IFOC technique is the most effective method for the control of the IM drive fed by voltage source inverter. In this paper, rotor oriented FOC method is implemented in both the DFOC and IFOC scheme of IM drive.

In the DFOC model, the sensor measures the rotor angular speed at the output data of the IM. In the IFOC scheme, also called as the sensor-less scheme, since one can't directly measure the rotor speed from the output of IM, a speed estimator is used which assess the rotor angular speed by using I_{abc} and V_{abc} from the inverter output and applied to the controller for dynamic performance of IM. In IFOC scheme, the model works with a calculated speed reference instead of an actual data from the motor output. Hence IFOC scheme eliminates most of the problems associated with the sensor. The electromagnetic torque ripples are relatively more in IFOC as compared to DFOC. The cost of IFOC scheme based IM drive is less as it is a sensor-less scheme. The total harmonic distortion is less in IFOC as compared to DFOC as shown in THD-FFT results. By analysis of speed, torque and stator current responses of the motor at different modes of operation, it is concluded that the IFOC system has better robustness, performance and stability than DFOC scheme by considering the simulation results.

VI. NOMENCLATURE

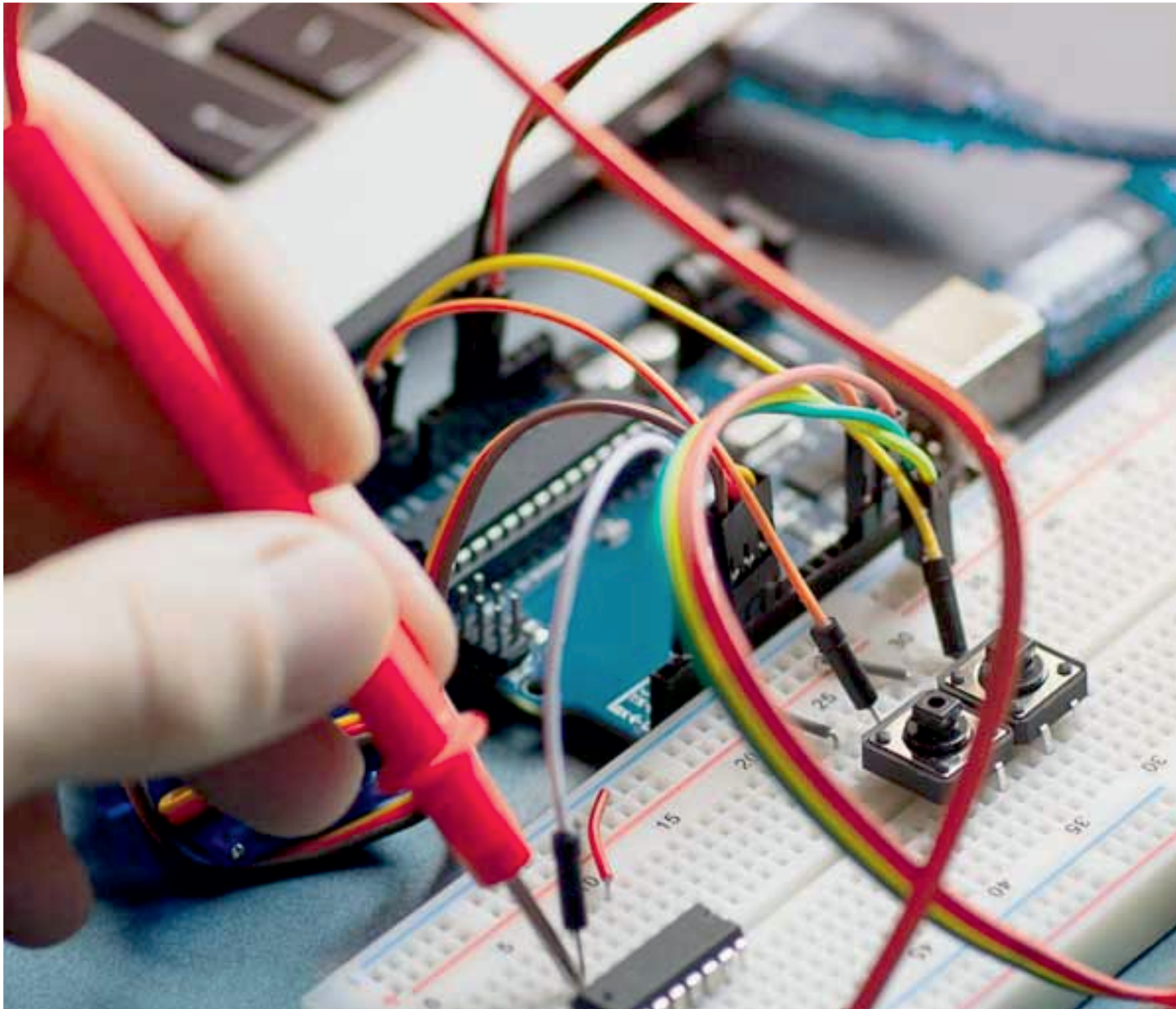
i_{ds}, i_{qs}	Stator current component in the stationary reference frame of d-q axes
i_{dr}, i_{qr}	Rotor current component in the stationary reference frame of d-q axes
R_s, R_r	Stator resistance and rotor resistance on IM
L_{ls}, L_{lr}	Leakage reactance of stator and rotor
L_s, L_r	Stator inductance and rotor inductance
L_m	Magnetizing inductance
V_{ds}, V_{qs}	Stator voltage component in the stationary reference frame of d-q axes
T_e	Electromagnetic torque of IM
ψ_{ds}, ψ_{qs}	Stator flux component of d-q axes reference frame
ψ_{dr}, ψ_{qr}	Rotor flux component of d-q axes reference frame
ω_s, ω_r	Stator and rotor angular speed
T_r	Rotor time constant
\mathcal{D}	Differential operator d/dt
ψ_{dr}^e, ψ_{qr}^e	d-q axes actual rotor flux
ψ_{dm}^s, ψ_{qm}^s	peak magnitude d-q axes of air-gap flux linkage in stationary reference frame

REFERENCES

1. Paul C. Krause, Oleg Wasynczuk, Scott D. Sudhoff, "Analysis of Electric Machinery and Drive Systems" 2nd Edition A John Wiley & Sons, INC. Publication, IEEE power series, pp. 525-554
2. Bimal K. Bose, "Modern Power Electronics and AC Drives" PH PTR, 2002.
3. Zhen Guo, Jiasheng Zhang, Zhenchuan Sun, Changming Zheng, "Indirect Field Oriented Control of Three-Phase Induction Motor Based on Current -Source Inverter," 13th Global Congress on Manufacturing and Management, GCMM 2016.



4. Saji Chacko, Dr. Chandrashekhara N. Bhende, Dr. Shailendra Jain, Dr. R. K. Nema, “Modeling and Simulation of Field Oriented Control Induction Motor Drive and Influence of Rotor Resistance Variations on Its Performance,” (ELELIJ) Vol. 5, No. 1, February 2016.
5. Ritu Tak, Sudhir Y Kumar, Bharat Singh Rajpurohit, “Estimation of Rotor and Stator Resistance for Induction Motor Drives using Second order of Sliding Mode Controller,” Journal of Engineering Science and Technology Review 10 (6) (2017) 9-15.
6. Darko P. Marcetic, Slobodan N. Vukosavic “Speed Sensorless AC Drives with the Rotor Time Constant Parameter Update” IEEE Transaction on industrial electronics, Vol.54, No.5, Oct 2007.
7. Colin Schauder, “Adaptive Speed Identification for Vector Control of Induction Motors without Rotational Transducers,” IEEE Transactions on Industry Applications, Vol. 28, No. 5, September/October 1992.
8. Venu Gopal B T, “Comparison Between Direct and Indirect Field Oriented Control of Induction Motor” (IJETT) – Volume-43 Number-6-January 2017.
9. Wei Li, Zhifeng Xu, Yulin Zhang, “Induction Motor Control System Based on FOC Algorithm,” 8th IEEE Joint International Information Technology and Artificial Intelligence Conference (ITAIC 2019).
10. Muawin A. Magzoub, Nordin B. Saad, Rosdiazli B. Ibrahim, “Analysis and Modeling of Indirect Field-Oriented Control for PWM-driven Induction Motor Drives,” 2013 IEEE Conference on Clean Energy and Technology (CEAT).
11. Mohamed Boussak, “A High-Performance Sensorless Indirect Stator Flux Orientation Control of Induction Motor Drive,” IEEE Transactions on Industrial Electronics, Vol. 53, No. 1, February 2006.



INNO  **SPACE**
SJIF Scientific Journal Impact Factor

Impact Factor:
7.122

ISSN INTERNATIONAL
STANDARD
SERIAL
NUMBER
INDIA



International Journal of Advanced Research

in Electrical, Electronics and Instrumentation Engineering

 **9940 572 462**  **6381 907 438**  **ijareeie@gmail.com**



www.ijareeie.com

Scan to save the contact details